Journal of Pharmaceutical and Biomedical Analysis 53 (2010) 567–575

Contents lists available at ScienceDirect

Journal of Pharmaceutical and Biomedical Analysis

journal homepage: www.elsevier.com/locate/jpba

Lipidomic metabolism analysis of the endogenous cannabinoid anandamide (N-arachidonylethanolamide)

Ekaterina A. Placzek[a], Bruce R. Cooper[b], Andrew T. Placzek[a], Julia A. Chester[c], V. Jo Davisson[a,b], Eric L. Barker[a,*]

[a] Department of Medicinal Chemistry and Molecular Pharmacology, Purdue University, 575 Stadium Mall Drive, West Lafayette, IN 47904, United States
[b] Bindley Bioscience Center, 1203 West State Street, West Lafayette, IN 47907, United States
[c] Department of Psychological Sciences, 703 Third Street, West Lafayette, IN 47904, United States

ARTICLE INFO

Article history:
Received 11 January 2010
Received in revised form 19 March 2010
Accepted 26 March 2010
Available online 1 April 2010

Keywords:
Anandamide
Arachidonic acid
Mass spectrometry
Argentation
Stable isotope encoding

ABSTRACT

Elucidation of pathways involved with lipid metabolism has been limited by analytical challenges associated with detection and structure identification. A discovery-based mass spectrometry lipidomic approach has been applied to identify metabolites of the endogenous cannabinoid anandamide (N-arachidonylethanolamide). Previously, a model system was established to show that anandamide can be recycled by cells to form new endocannabinoids suggesting recycling of the arachidonate carbon chain. We hypothesized that distinct cellular pathways exist to direct the anandamide-derived arachidonate chain into a specific set of metabolites, different from the metabolite pool that is comprised of non-anandamide-derived arachidonic acid. Using stable isotope encoding and liquid chromatography–mass spectrometry, we identified a distinct pool of lipid metabolites derived from exogenous anandamide or arachidonic acid in RBL-2H3 cells. We discovered that arachidonic acid-derived metabolites were primarily comprised of the eicosanoid lipid class, whereas anandamide-derived arachidonic acid, in addition to eicosanoids, was metabolized into diradylglycerols, fatty acid amides, sterols, and glycerophospholipids. From the list of anandamide metabolites of particular interest was 1-*O*-arachidonyl-*sn*-glycero-3-phosphocholine. Furthermore, we determined that while 1-*O*-arachidonyl-*sn*-glycero-3-phosphocholine may be a metabolite of anandamide, the *sn*-2 compound was more abundant in mouse brain tissue. Overall, our results provide a novel approach to study the metabolic fate of endocannabinoids and fatty acid-derived signaling molecules.

1. Introduction

Lipidomic approaches provide a new opportunity to explore the biology of hydrophobic molecules such as fatty acids. Analysis of metabolism using lipidomics can assist in the discovery of new pathways involved in the biotransformation of lipid-derived signaling molecules. Such pathways can be explored as potentially novel targets for pharmacological manipulation. We have been particularly interested in the metabolism of the endogenous cannabinoids such as anandamide (AEA) and 2-arachidonylglycerol (2-AG). These endocannabinoids mimic the actions of the main active ingredient in marijuana Δ^9-tetrahydrocannabinol (Δ^9-THC) and produce pharmacologic effects similar to plant-derived cannabinoids [1,2].

AEA, 2AG, as well as Δ^9-THC target the G protein-coupled CB1 and CB2 cannabinoid receptors [1,2]. AEA has also been shown to have agonist activity at the vanilloid receptor (VR1) that is a member of the transient receptor potential (TRP) superfamily of ion channels [3,4]. Both AEA and 2-AG have been linked to retrograde signaling in the CNS [5]. Additionally, endocannabinoids modulate many diverse biological targets, and therefore may play a role in physiological processes such as pain, nausea, reproduction, immune response, and cancer [6,7]. Characterization and pharmacologic manipulation of the endocannabinoid system offers potential avenues for dietary or therapeutic intervention in many disorders without the undesirable psychotropic side effects that plant-derived cannabinoids produce.

The profiles of 2-AG and AEA inactivation are similar and cellular uptake of these molecules result in signal termination [8]. Our previous efforts demonstrated that AEA uptake may occur via a non-clathrin-mediated endocytic process that is rapid, saturable, and temperature-dependent [9,10]. The identity of the protein(s) involved in the transport of both 2-AG and AEA, however, is not known. Following uptake, 2-AG may be hydrolyzed either by fatty acid amide hydrolase (FAAH) or monoacylglycerol lipase to yield arachidonic acid (ARA) and glycerol, whereas AEA is hydrolyzed by FAAH into ARA and ethanolamine [11–15]. However, there is also

* Corresponding author. Tel.: +1 765 494 9940; fax: +1 765 494 1414.
E-mail address: barkerel@purdue.edu (E.L. Barker).

0731-7085/$ – see front matter © 2010 Elsevier B.V. All rights reserved.
doi:10.1016/j.jpba.2010.03.035

clear evidence that AEA and 2-AG may be metabolized by other enzymes as well leading to a variety of lipid species, some of which may have significant biological activity [16–19].

Although many other pathways have been identified that may contribute to the biotransformations of AEA, the extent to which these pathways may be involved is not completely understood. Single pathway analysis using conventional approaches limits the ability to explore these alternative pathways. Therefore, in order to improve our understanding of endocannabinoid biology, new high content approaches examining multiple metabolic pathways would be useful.

An approach to study and identify new pathways and their constituent protein components can involve tracking the metabolic fate of fatty acid chain pools derived from endocannabinoids. We previously discovered that AEA metabolites, ARA and ethanolamine, are trafficked to the plasma membrane accumulating in the lipid raft microdomain region of the cell [9]. Lipid rafts are specialized microdomains in the plasma membrane that are enriched in ARA, cholesterol, plasmenylethanolamine, and sphingolipids [20,21]. Furthermore, RBL-2H3 cells were discovered to recycle the arachidonate chain derived from exogenous AEA to form new AEA and 2-AG molecules, a process we refer to as endocannabinoid recycling [22].

In order to detect AEA and 2-AG molecules from RBL-2H3 cells, we previously used thin-layer chromatography (TLC) analysis [22]. The drawback of this method is that even though the detection of AEA and 2-AG is achieved without difficulty, a profile of metabolites is not easily resolved or characterized. We propose that pathways may exist to direct the AEA-derived arachidonate chain into a set of metabolites that may differ from the metabolite pool that is comprised of non-AEA-derived ARA. In the present study, we focused on identifying low molecular weight lipid molecules that arise from AEA and ARA metabolism in cells.

The cellular metabolites of AEA and ARA were pursued by the use of a mass spectrometry method using silver coordination to the arachidonate backbone of AEA and ARA and the metabolite species were analyzed using liquid chromatography–mass spectrometry (LC–MS). Accurate mass measurement capabilities were enhanced by the use of a quadrupole time-of-flight (Q-TOF) instrument. A major technical issue in LC–MS analysis of lipids, i.e. poor ionization efficiency of endocannabinoid molecules, was overcome by adding silver to the mobile phase [23]. Once validated, the mass spectrometry method was employed with a stable isotope encoding approach to study the metabolites of AEA and identify species into which the arachidonate backbone derived from AEA or ARA incorporated. The accurate mass measurement of the Q-TOF instrument in concert with enhanced sensitivity introduced by using silver provided us with a unique method to identify lipid molecules. The method should be readily applied as a discovery tool to study various small molecules, containing double bonds with partially unfilled d-orbitals, that poorly ionize under standard conditions in mass spectrometry analysis. Furthermore, the results of this study may provide new opportunities to study the unique pattern of molecules associated with various physiological events that endocannabinoids modulate.

2. Experimental

2.1. HPLC/MS analysis

The LC/MS method was based on the protocol by Kingsley and Marnett, with some modifications [23]. The chromatography was conducted on a Waters Alliance 2795 HPLC system (Milford, MA, USA). Separation was performed using a Thermo HyPurity Advance column (100 mm × 2.1 mm, 3 μm), maintained at a temperature of 35 °C and a flow rate of 0.3 ml/min. The mobile phase contained solvents A and B, where A was 70 μM silver acetate in water and B was 70 μM silver acetate in a 90% methanol 10% water solution. The gradient began with a 1 min hold at 55% B, increased linearly to 99% B at 13 min, was held at 99% B for 2 min, and returned to the original composition of 55% B composition at 16 min. The column was equilibrated back to the initial conditions between injections for 6 min.

The HPLC system was coupled to a Micromass QTof-micro (Manchester, UK) mass spectrometer equipped with an electrospray source operated in positive ion mode. Source parameters were optimized to maximize the detection of AEA. The instrument was mass calibrated against a sodium formate reference solution prior to each use. The source temperature was set at 120 °C with a cone gas flow of 50 L/h, a desolvation gas temperature of 350 °C, and a nebulization gas flow of 700 L/h. The capillary voltage was set at 3.5 kV and the cone voltage to 35 V. A scan time of 960 ms with an inter-scan delay of 100 ms was used. Data were collected from m/z 100–1000 in continuum mode, using Waters MassLynx (v. 4.0 SP4) software. The quantification method for AEA and 2-AG was validated over the range 0.014–1.4 μM by demonstrating appropriate standard curve fit (quadratic, $n = 7$, $R^2 = 0.994$), precision ($n = 5$, RSD = 3.1%), limit of detection (15 fmol injected), and recovery (spiked standard greater than 75%).

LC/MS/MS was performed as above, using argon as the collisionally induced dissociation gas at 22 eV. Lock mass correction was utilized using reserpine at a defined mass of 609.2807 amu.

2.2. Labeling of the lipid metabolites

RBL-2H3 cells, maintained in DMEM with 5% fetal clone I and 5% bovine calf serum supplemented with 2 mM L-glutamine and 1% penicillin/streptomycin in a CO_2-containing (5%) humidified environment at 37 °C, were plated in 150-mm tissue culture plates. Twenty-four hours after plating, one population of cells was treated with normal isotopic abundance AEA (10 μM) and the other with deuterated d_8-AEA (10 μM) (deuterium atoms at the 5, 6, 8, 9, 11, 12, 14, and 15 positions; Cayman Chemical, Ann Arbor, MI). Each population was grown for the next 24 h at 37 °C, allowing the endocannabinoid species to metabolize and incorporate into the cellular lipid pools. In the experiment that was designed to evaluate ARA metabolites, RBL-2H3 cells were treated with 10 μM ARA or 10 μM deuterated (d_8)-ARA (deuterium atoms at the 5, 6, 8, 9, 11, 12, 14, and 15 positions; Cayman Chemical, Ann Arbor, MI). For the assay, cells were washed twice with Krebs-Ringer Hepes (KRH) buffer (120 mM NaCl, 4.7 mM KCl, 1.2 mM KH_2PO_4, 1.2 mM $MgSO_4$, 10 mM Hepes and 2.2 mM $CaCl_2$, pH 7.1) at 37 °C with 0.5% fatty acid free BSA and once with KRH buffer without BSA. KRH buffer without BSA was then added to each plate, and the cells were incubated at 37 °C for 10 min. In the experiment that evaluated how metabolite pools change upon stimulation, the cells pre-labeled with deuterated lipids were stimulated with ionomycin (1 μM, 10 min 37 °C) while cells pre-labeled with non-deuterated lipids were treated with buffer control. In both cases, the assay buffer was discarded after the incubation, 1 mL of 1:1 mixture of cold methanol and acetonitrile was immediately added to each sample, and cells were scrapped off the plate. Next both of the cell populations, containing light (control) and heavy (stimulated) isotopes were mixed together. The resulting samples were maintained on ice and homogenized using a Dounce homogenizer (Wheaton, Millville, NJ). The homogenates were centrifuged for 20 min at 40,000 × g at 4 °C. Supernatants were collected, and the solvent was evaporated under a stream of argon. Once all solvent was evaporated, 40 μL of methanol was added to the samples, vortexed for 1 min, and submitted for mass spectrometric analysis. LC–MS analysis was performed, injecting 15 μL from each sample.

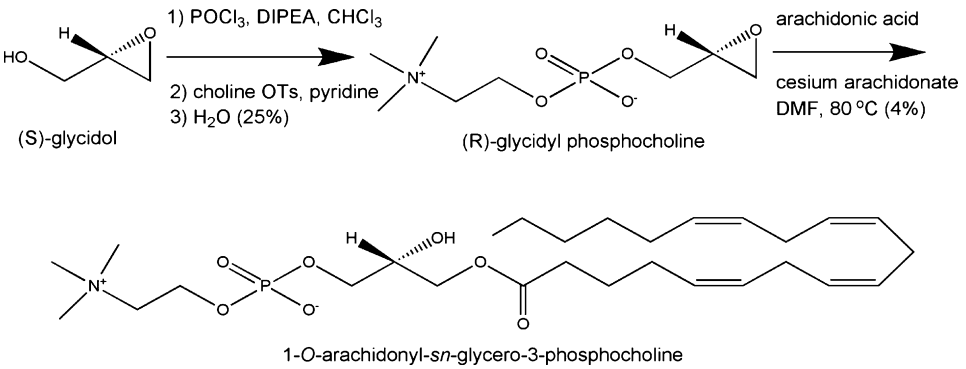

Fig. 1. Synthetic scheme for the synthesis of 1-*O*-arachidonyl-*sn*-glycero-3-phosphocholine, modified from a published protocol by Lindberg and colleagues [25].

The metabolites into which the arachidonate backbone was incorporated were represented as doublets (pairs of peaks corresponding to the light and heavy lipid isotopes) in the LC/MS. The doublets were identified using XMASS, a software program capable of identifying doublets in LC/MS data [24]. All data were acquired in profile mode, converted to centroid format, and transported to XMASSS in netCDF format. The results generated after XMASS processing provided a list of all chromatographic peaks whose spectra showed doublets that differed by 8 mass units, the ratio between the two isotopes, and the retention time for each species. Because the untreated RBL-2H3 samples should contain nearly equal amounts of AEA and d_8-AEA-derived species, we selected those doublets from the XMASS output files that contained isotopic ratios no greater than two. Using a lipid database, Lipid Metabolites and Pathways Strategy (Lipid MAPS, http://www.lipidmaps.org), preliminary identities for each doublet were assigned based upon the molecular weights provided in the output file. Searches were conducted using a mass range of ±0.3 amu.

2.3. Synthesis of 1-O-arachidonyl-sn-glycero-3-phosphocholine

Synthesis of 1-*O*-arachidonyl-*sn*-glycero-3-phosphocholine (Fig. 1) was carried out with slight modifications from the published procedure [25]. To a stirred solution of (*S*)-glycidol (Sigma, 670 mg, 9.04 mmol) and ethyl N,N-diisopropylamine (Sigma, 6.5 mL, 9.5 mmol) in chloroform (20 mL) at 0 °C under an argon atmosphere was added phosphorus oxychloride (Sigma, 1.40 g, 9.13 mmol). After 2 h, pyridine (2.0 mL) and choline tosylate (Sigma, 2.89 g, 10.5 mmol) were added, and the mixture was allowed to attain room temperature. After an additional 5 h, water was added (0.50 mL), and the stirring was continued for 1 more hour. Ethanol was added to the reaction mixture, resulting in a 70% EtOH solution. Concentration and flash chromatography (70% EtOH) provided (*R*)-glycidyl phosphocholine (550 mg, 2.30 mmol, 25%). R_f = 0.19 (70% EtOH); ^{1}H NMR was identical to that previously published (Supplementary Fig. 1) [25]. Cesium carbonate (54 mg) was mixed with arachidonic acid (50 mg) in 2 mL of DMF. (*R*)-glycidyl phosphocholine (20 mg, 0.0821 mmol) was added to the cesium arachidonate mixture and stirred at 80 °C. After 26 h, the mixture was loaded onto a silica gel column and run with a methanol:H_2O (5:1) solution to give an oily 1-*O*-arachidonyl-*sn*-glycero-3-phosphocholine (2 mg, 0.0036 mmol, 4%), R_f 0.29 (MeOH/H_2O 5:1).

2.4. Detection of AEA, 2-AG, and 1-O-arachidonyl-sn-glycero-3-phosphocholine in mouse brain tissue

Mouse brain samples were prepared for analysis of endocannabinoids using a protocol developed by Bradshaw and colleagues [26]. Tissue was immediately frozen at −80 °C upon sacrificing, stored at −80 °C, allowed to thaw on ice for 1 h, and weighed. Post-mortem changes in endocannabinoid levels have been well documented [27,28]. We performed stability experiments that revealed the 1 h thaw on ice does not alter 2-AG levels, but may result in ∼20% loss of AEA (data not shown). Twenty volumes of 1:1 mixture of cold methanol and acetonitrile were added to each tissue sample. The samples were maintained on ice and homogenized using a Polytron homogenizer (Kinematica). The homogenates were centrifuged for 20 min at 40,000 × *g* at 4 °C. Supernatants were collected and transferred to 15 mL polypropylene centrifuge tubes. HPLC-grade water was added to each sample to create a 70:30 (water:organic) solution. A deuterated AEA standard (100 pmol in 15 μL) was added to each sample as an internal standard to track the recovery of the test compounds. Analytes were extracted from the supernatant using C18 solid-phase extraction (SPE) columns (Bond Elut 500 mg, Varian). The SPE columns were conditioned with 2.5 mL methanol and equilibrated with 2 mL water, followed by sample loading. The SPE columns were then washed with 2 mL water and 1.5 mL 55% methanol, followed by elution with 1 mL methanol. Each eluate was dried, reconstituted in 40 μL methanol, and vortexed for 1 min. LC–MS analysis was performed, injecting 15 μL from each sample. Quantitation in brain samples was performed using standard curves, ranging from 0.014 to 1.4 μM for AEA and 2-AG, and 0.30 to 368 μM for 1-*O*-arachidonyl-*sn*-glycero-3-phosphocholine.

3. Results

3.1. Coordination of silver cations to endocannabinoids improves detection capabilities by Q-TOF mass spectrometry

In the present study, an LC–MS-based approach was developed in order to investigate the endocannabinoid metabolome in addition to the two predominant endogenous compounds, AEA and 2-AG. A Q-TOF mass spectrometer used in these experiments provided suitable levels of mass accuracy to make initial predictions of endocannabinoid metabolite identities based on molecular weights. We discovered that silver coordination to the arachidonate backbones of AEA and 2-AG [23] improved the detection of the Q-TOF mass spectrometer. Instead of quantifying compound levels using the $[M+H]^+$ peaks, the more prominent $[M+^{107}Ag]^+$ and/or $[M+^{109}Ag]^+$ ions were used to quantify the molecules of interest (Fig. 2). This method allowed us to quantify (signal-to-noise >10) AEA at a concentration of 1.44 pmol/mL and 2-AG at 2.1 pmol/mL, representing an improvement in sensitivity of 30-fold when compared to attempts without the inclusion of silver ion. Furthermore, the limit of detection could be extended to 15 fmol on column for both species, values consistent with other published reports [23,29].

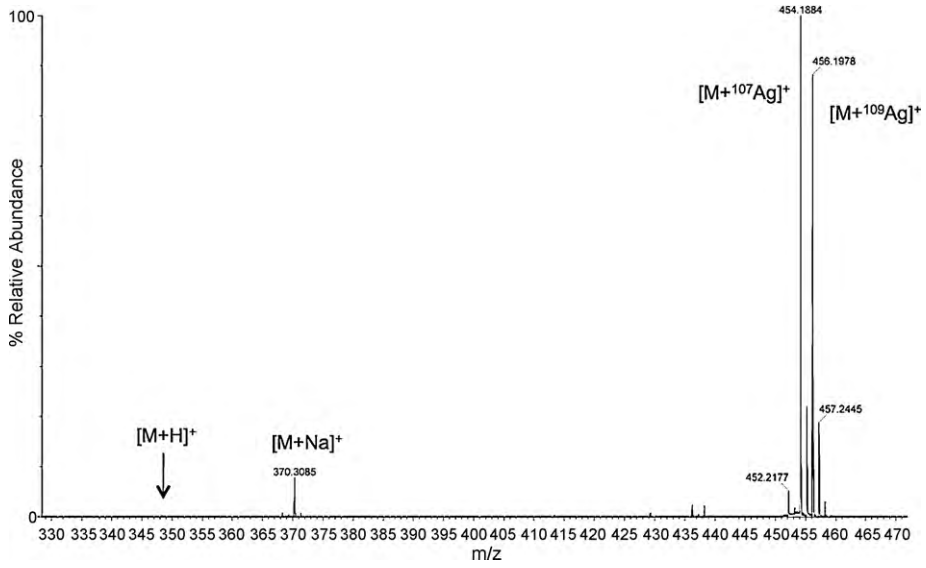

Fig. 2. Silver coordination to the arachidonate backbones of endocannabinoids significantly improves the detection of AEA. Mass spectrum of a 0.72 μM AEA standard displays the relative intensities of the AEA peaks observed in the presence of silver ion in ESI positive mode: $[M+H]^+$ at *m*/*z* 348.3, $[M+Na]^+$ at *m*/*z* 370.3, $[M+^{107}Ag]^+$ at *m*/*z* 454.2, and $[M+^{109}Ag]^+$ at *m*/*z* 456.2.

3.2. AEA and 2-AG are detected in mouse brain tissue using the new argentation MS method

Once the method using AEA and 2-AG standards was developed, quantification of endocannabinoids in a biological context was pursued. The AEA and 2-AG in mouse brain tissue was quantified (Table 1) and on average, 10.6 pmol/g of AEA and 1133.5 pmol/g 2-AG in whole mouse brains were estimated which are values consistent with the results of other studies [26,30]. Furthermore, the amount of 2-AG found in brain tissue exceeds that of AEA by approximately 150-fold [31–33]. Our results indicated that the concentration of 2-AG in mouse brain was approximately 110 times higher than that of AEA. We did observe a minor peak (<20%) partially co-eluting with 2-AG. This minor peak is consistent with 1-AG that is most likely the result of interconversion from 2-AG, thus, the results represent summed values for the 2-AG and 1-AG peaks. It should also be noted that the standard curves used for quantification were not generated in the context of a biological matrix, so the absolute values should be viewed as relative concentrations. However, this limitation should not alter the interpretation of our results. These results establish that the silver ion enhancement for endocannabinoid ionization combined with the Q-TOF analyzer can achieve equivalent results to those of the triple quadrupole mass spectrometer.

3.3. AEA-derived ARA is incorporated into a distinct pool of metabolites

The stable isotope encoding approach was used to study AEA recycling and applied to the identification of metabolite species containing the exogenous arachidonate backbone derived from AEA or ARA. The technique of isotope encoding relies on the principle that molecules with the same chemical structure, differing only in their isotopic composition, will be processed by cells in a similar manner and respond equally when analyzed simultaneously using a mass spectrometer. Metabolic labeling involves two populations of cultured cells treated with isotopically distinct species that are otherwise structurally identical. Both of the cell populations, pre-labeled with light and heavy isotopes, are mixed in equal proportions. During the chromatographic analysis, both isotopes will elute with essentially the same retention time. However, in the mass spectrum a set of doublets will be produced. In these experiments, doublets are pairs of mass peaks that correspond to the light and heavy isotopes and differ from each other by eight mass units, i.e. the mass of the deuteriums that are present in the d_8-AEA-coded sample, and share the same chromatographic retention time.

RBL-2H3 cells are a cognate mast cell line that has been successfully used to study AEA uptake and biosynthesis [9,34,35]. The AEA metabolite pool was encoded with either the light- or deuterium-substituted arachidonate carbon chain using either 10 μM AEA or d_8-AEA to pre-label cells at a concentration close to the apparent K_m value for uptake in RBL-2H3 cells and the K_m for FAAH [36]. After the samples were mixed and mass analyzed, the output data file was formatted and processed by XMASS software to create a peak list. From the list of doublets, those pairs that had a ratio that was no greater than 2 were selected. The doublets reported represent an analysis of three separate experiments; thus, the identified peaks were reproducible across all three experiments using the described criteria. Analysis of technical replicates in the doublet experiments suggests that the ratios for doublet peak intensities have a standard deviation of 0.165. Our approach may result in some false negatives, but minimizes false positives. The results were then also compared to the peaks generated from untreated cell samples which provided a baseline level for the observed peaks. Any doublet appearing in the untreated cell sample alone was removed from the XMASS output file and treated as a background doublet. The differential isotope encoding method proved to be an effective means to compare the lipid population of metabolites between two samples simultaneously. This approach allowed us to discover a set of AEA-derived arachidonate-containing metabolites that were detected in ESI+ mode (Table 2). Forty different lipid species were detected in

Table 1
The levels of AEA, 2-AG, and 2-*O*-arachidonyl-*sn*-glycero-3-phosphocholine in mouse brain as detected with LC–MS (average ± S.D.). For AEA and 2-AG $n = 6$, for 2-*O*-arachidonyl-*sn*-glycero-3-phosphocholine $n = 3$.

Molecule name	Amount detected in brain tissue
AEA	10.6 ± 3.3 pmol/g
2-AG	1133.5 ± 269 pmol/g
2-*O*-arachidonyl-*sn*-glycero-3-phosphocholine	52.9 ± 3.9 nmol/g

Table 2
A list of proposed AEA-derived metabolites. Stable isotope encoding experiments examining AEA-derived metabolites were performed in RBL-2H3 cells as described in Section 2. Using a lipid database Lipid Metabolites and Pathways Strategy (Lipid MAPS, http://www.lipidmaps.org), we determined a possible identity of doublets based on the molecular weight that was provided in the output file. (–) means that no lipid molecule at that particular molecular weight was identified in the database. The unlabeled control samples provide a comparison as to whether the observed peak in the labeled samples (AEA or d_8-AEA) was less than (<), greater than (>), or equal to (=) the corresponding peak in the unlabeled control.

Retention time range (min)	Molecular weight	Comparison to unlabeled control	Proposed identity of AEA-derived metabolites
11.50–12.45	343.71	<	–
9.03–9.44	347.19	>	Sodium 4R,12S-dihydroxy-9-oxo-5E,7E,10Z,13Z-prostatetraenoate-cyclo[8,12]
	347.28		N-(7Z,10Z,13Z,16Z-docosatetraenoyl)-ethanolamine
9.14–9.40	359.32	>	N-butyl-5Z,8Z,11Z,14Z-eicosatetraenoyl amine
			N,N-diethyl-5Z,8Z,11Z,14Z-eicosatetraenoyl amine
			N-tert-butyl-5Z,8Z,11Z,14Z-eicosatetraenoyl amine
			N-propyl-2-methyl-5Z,8Z,11Z,14Z-eicosatetraenoyl amine
			N-(1R-methyl-propyl)-5Z,8Z,11Z,14Z-eicosatetraenoyl amine
			N-isopropyl-2-methyl-5Z,8Z,11Z,14Z-eicosatetraenoyl amine
			N-(1S-methyl-propyl)-5Z,8Z,11Z,14Z-eicosatetraenoyl amine
7.31–7.69	366.20	=	5S,12R-dihydroxy-6Z,8E,10E,14Z-eicosatetraene-1,20-dioic acid
12.42–12.72	371.28	=	N-(4Z,7Z,10Z,13Z,16Z,19Z-docosahexaenoyl)-ethanolamine
4.29–4.56	372.19	=	9-Oxo-12S-acetoxy-5Z,7E,10Z,14Z-prostatetraenoic acid-1,4R-lactone-cyclo[8,12]
			9-Oxo-12S-acetoxy-5E,7Z,10Z,14Z-prostatetraenoic acid-1,4R-lactone-cyclo[8,12]
			9-Oxo-12S-acetoxy-5E,7E,10Z,14Z-prostatetraenoic acid-1,4R-lactone-cyclo[8,12]
10.3–10.4	375.31	=	N-(1,1-dimethy-2-hydroxy-ethyl)-5Z,8Z,11Z,14Z-eicosatetraenoyl amine
			N-(2,2-dimethy-5Z,8Z,11Z,14Z-eicosatetraenoyl)-ethanolamine
			N-ethyl-N-(2-hydroxy-ethyl)-5Z,8Z,11Z,14Z-eicosatetraenoyl amine
			N-(5Z,8Z,11Z,14Z-docosatetraenoyl)-ethanolamine
8.71–9.06	390.20	=	5S,12R-dihydroxy-20,20,20-trifluoro-6Z,8E,10E,14Z-eicosatetraenoic acid
9.77–10.30	411.29	=	–
6.43–7.27	446.23	=	Methyl 4R,12S-diacetoxy-9-oxo-5Z,7E,10Z,13Z-prostatetraenoate-cyclo[8,12]
			Methyl 4R,12S-diacetoxy-9-oxo-5Z,7Z,10Z,13Z-prostatetraenoate-cyclo[8,12]
			Methyl 4R,12S-diacetoxy-9-oxo-5E,7E,10Z,13Z-prostatetraenoate-cyclo[8,12]
			Methyl 4S,12S-diacetoxy-9-oxo-5E,7E,10Z,13Z-prostatetraenoate-cyclo[8,12]
			Methyl 4R,12S-diacetoxy-9-oxo-5E,7Z,10Z,13Z-prostatetraenoate-cyclo[8,12]
			Methyl 4S,12S-diacetoxy-9-oxo-5E,7Z,10Z,13Z-prostatetraenoate-cyclo[8,12]
12.16–12.70	476.80	=	–
9.71–10.55	492.38	=	–
7.28–7.63	534.99	=	–
7.99–8.11	543.33	=	1-(5Z,8Z,11Z,14Z-eicosatetraenoyl)-*sn*-glycero-3-phosphocholine
9.94–10.39	554.92	=	–
9.00–9.83	557.92	=	–
10.33–10.63	563.53	<	–
9.95–10.54	580.81	=	–
11.58–11.34	592.41	>	–
10.63–10.92	598.09	=	–
10.35–10.74	605.57	=	–
10.12–10.88	609.55	=	–
14.20–14.56	614.49	<	1-(9Z,12Z-octadecadienoyl)-2-(9Z,12Z,15Z-octadecatrienoyl)-*sn*-glycerol
			1-Hexadecanoyl-2-(5Z,8Z,11Z,14Z,17Z-eicosapentaenoyl)-*sn*-glycerol
7.26–7.63	622.61	=	–
11.45–11.47	628.51	<	1-(9Z-heptadecenoyl)-2-(5Z,8Z,11Z,14Z-eicosatetraenoyl)-*sn*-glycerol
			1-Heptadecanoyl-2-(5Z,8Z,11Z,14Z,17Z-eicosapentaenoyl)-*sn*-glycerol
15.19–15.69	646.25	<	–
14.04–14.12	647.71	<	–
7.22–7.63	667.13	=	–
9.79–9.92	668.54	=	1-(11Z,14Z-eicosadienoyl)-2-(5Z,8Z,11Z,14Z-eicosatetraenoyl)-*sn*-glycerol
			1-(11Z-eicosenoyl)-2-(5Z,8Z,11Z,14Z,17Z-eicosapentaenoyl)-*sn*-glycerol
			1-(9Z,12Z-octadecadienoyl)-2-(7Z,10Z,13Z,16Z-docosatetraenoyl)-*sn*-glycerol
			1-Octadecanoyl-2-(4Z,7Z,10Z,13Z,16Z,19Z-docosahexaenoyl)-*sn*-glycerol
13.89–14.36	673.26	<	–
10.54–10.89	676.05	=	–
15.02–15.47	682.55	=	1-Nonadecanoyl-2-(4Z,7Z,10Z,13Z,16Z,19Z-docosahexaenoyl)-*sn*-glycerol
15.04–15.51	683.33	=	–
14.68–15.11	688.51	<	1-(5Z,8Z,11Z,14Z,17Z-eicosapentaenoyl)-2-(7Z,10Z,13Z,16Z,19Z-docosapentaenoyl)-*sn*-glycerol
			1-(5Z,8Z,11Z,14Z-eicosatetraenoyl)-2-(4Z,7Z,10Z,13Z,16Z,19Z-docosahexaenoyl)-*sn*-glycerol
14.67–14.55	689.31	<	–
14.49–14.91	702.30	<	–
14.67–15.17	704.57	<	Cholest-5-(15S-hydroperoxy-5Z,8Z,12E,14Z-eicosatetraenoate)
15.19–15.33	726.62	=	1-(13Z-docosenoyl)-2-(7Z,10Z,13Z,16Z-docosatetraenoyl)-*sn*-glycerol
			1-Docosanoyl-2-(7Z,10Z,13Z,16Z,19Z-docosapentaenoyl)-*sn*-glycerol
14.88–15.31	731.06	<	–

the AEA metabolite pool in the RBL-2H3 cells. Of those species, seventeen matched molecular weights of a specific lipid or lipid class in the Lipid MAPS database. The main classes of lipids that comprise the AEA metabolite pool are eicosanoids, diradylglycerols, fatty acid amides, sterols, and glycerophospholipids.

By applying the stable isotope encoding approach to compare the lipid metabolites that are produced from exogenous ARA to those from AEA-derived ARA, the classes of lipids involved in AEA recycling were found to be more diverse than those lipid metabolites derived from ARA. We hypothesized that cells utilize directed

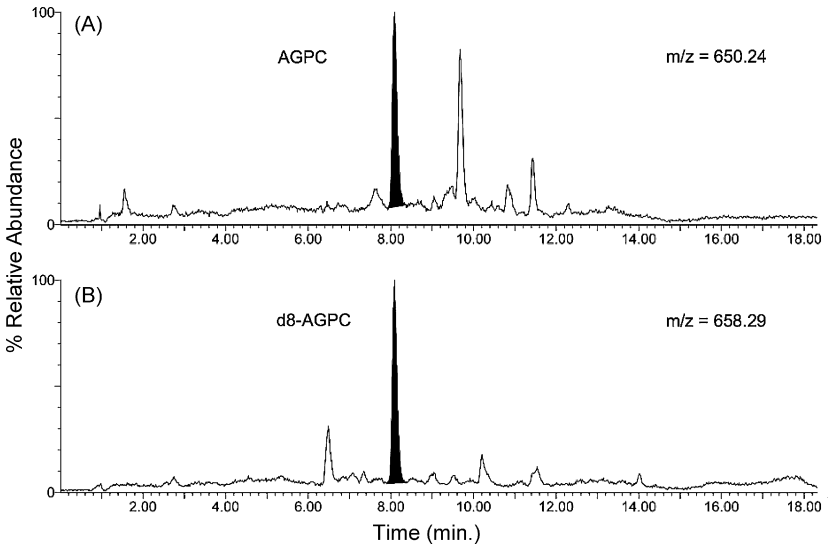

Fig. 3. A pair of doublet peaks in RBL-2H3 cells identified by XMASS as having a mass difference of 8 amu. A lipid database search proposed an identity of 1-*O*-arachidonyl-*sn*-glycero-3-phosphocholine (AGPC), a potential metabolite of AEA. (A) Selected ion chromatogram at 650.24 amu, with the highlighted peak of area 251.01 a.u. (B) Selected ion chromatogram at 658.29 amu, with the highlighted peak of area 323.25 a.u.

trafficking of lipids based on the source of the lipid. In other words, the AEA-derived arachidonate carbon chain may be directed into a different pool of metabolites compared with exogenous ARA, or ARA derived from any other lipid. The doublets were identified that corresponded to the metabolites of exogenously applied ARA and d_8-ARA. In contrast to the AEA metabolites, which comprised a wide variety of lipid classes, the ARA metabolite pool detected in this assay was limited (Supplemental Table 1) with the only class being identified as eicosanoids.

3.4. 1-O-arachidonyl-sn-glycero-3-phosphocholine is a metabolite of AEA

From the list of AEA metabolites that were identified using the LipidMAPS database, several species were of interest due to potential links to the endocannabinoid system. One of these molecules was a phosphocholine lipid, 1-*O*-arachidonyl-*sn*-glycero-3-phosphocholine (Table 1, 1-(5Z,8Z,11Z,14Z-eicosatetraenoyl)-*sn*-glycero-3-phosphocholine; Figs. 1 and 3). The lipid structure was comprised of a phosphocholine moiety coupled to an arachidonate carbon chain. To confirm the identity of the 1-*O*-arachidonyl-*sn*-glycero-3-phosphocholine molecule as an AEA metabolite, 1-*O*-arachidonyl-*sn*-glycero-3-phosphocholine was synthesized as a standard (Fig. 1). The mass spectrometric properties of this molecule were analyzed. The structure was confirmed by NMR (Supplemental Fig. 1) and LC/MS/MS spectrometry (Fig. 4B).

Mass spectrometry was used to verify the molecular weight and retention time of the doublet observed in our encoding experiments (Fig. 3). The major peak for the 1-*O*-arachidonyl-*sn*-glycero-3-phosphocholine standard eluted at 8.02 min, a retention time that matched the retention time of the proposed 1-*O*-arachidonyl-*sn*-glycero-3-phosphocholine that was selected from the list of doublets generated from isotope encoding experiments. Interestingly, the chromatogram for our synthesized standard showed two partially co-eluting peaks (7.78 and 8.02 min) (Fig. 4B). MS/MS analysis of the two peaks in the standard revealed the same fragmentation pattern but with differing ratios of the product ion intensities (Fig. 4D and E). We believe the major peak (8.02 min) represents the expected *sn*-1 regioisomer, but that the minor peak (7.78 min) represents a minor product corresponding to the *sn*-2 compound.

Finally, we examined if 1-*O*-arachidonyl-*sn*-glycero-3-phosphocholine occurs endogenously in the CNS. Whole mouse brain tissue was extracted and analyzed for the presence of 1-*O*-arachidonyl-*sn*-glycero-3-phosphocholine. The brain sample showed a single predominant peak with some broadening that had a similar retention time (7.8 min) and *m*/*z* value as the synthesized standard (Fig. 4A and B). Further confirmation was obtained by generating a collisionally induced dissociation spectrum for the peak in the brain tissue. The relative intensities of the product ions observed in the MS/MS analysis of the brain sample peak (Fig. 4C) supports identification of the brain product as 2-*O*-arachidonyl-*sn*-glycero-3-phosphocholine, not 1-*O*-arachidonyl-*sn*-glycero-3-phosphocholine (Fig. 4E). Using the same methods described above, the phosphocholine molecule was determined to be present in mouse brain tissue at 52.9 nmol/g (Table 1).

4. Discussion

Novel endocannabinoid molecules and their metabolites are receiving attention due to their potential to regulate the classical cannabinoid physiology. Detection of the complete family of endocannabinoid-related metabolites produced *in vivo* and characterization of enzymes involved with such biotransformations is crucial for the characterization of the endocannabinoid system, and may allow for identification of other compounds that modulate the signaling of both AEA and 2-AG as well as their targets. We have previously demonstrated that RBL-2H3 cells recycle the arachidonate chain derived from [^{3}H] AEA into new AEA molecules [22]. In addition, AEA-derived 2-AG synthesis and release was also observed in RBL-2H3 cells in response to ionomycin [22]. Therefore, we concluded that the arachidonate chain derived from AEA may be recycled by cells to form new endocannabinoid molecules. Our previous findings suggest that the AEA-derived arachidonate chain may be trafficked to and stored in specific regions of the cell, such as lipid raft microdomains [22]. Lipid raft microdomain organization may play a key role in endocannabinoid biosynthesis, because when these microdomains are disrupted, a decrease in endocannabinoid biosynthesis and release is observed [22]. Furthermore, RBL-2H3 cells recycle exogenous [^{3}H] ARA into new AEA and 2-AG molecules in response to ionomycin [22]. Interestingly, AEA and 2-AG synthesis is greater when the cells are pre-labeled

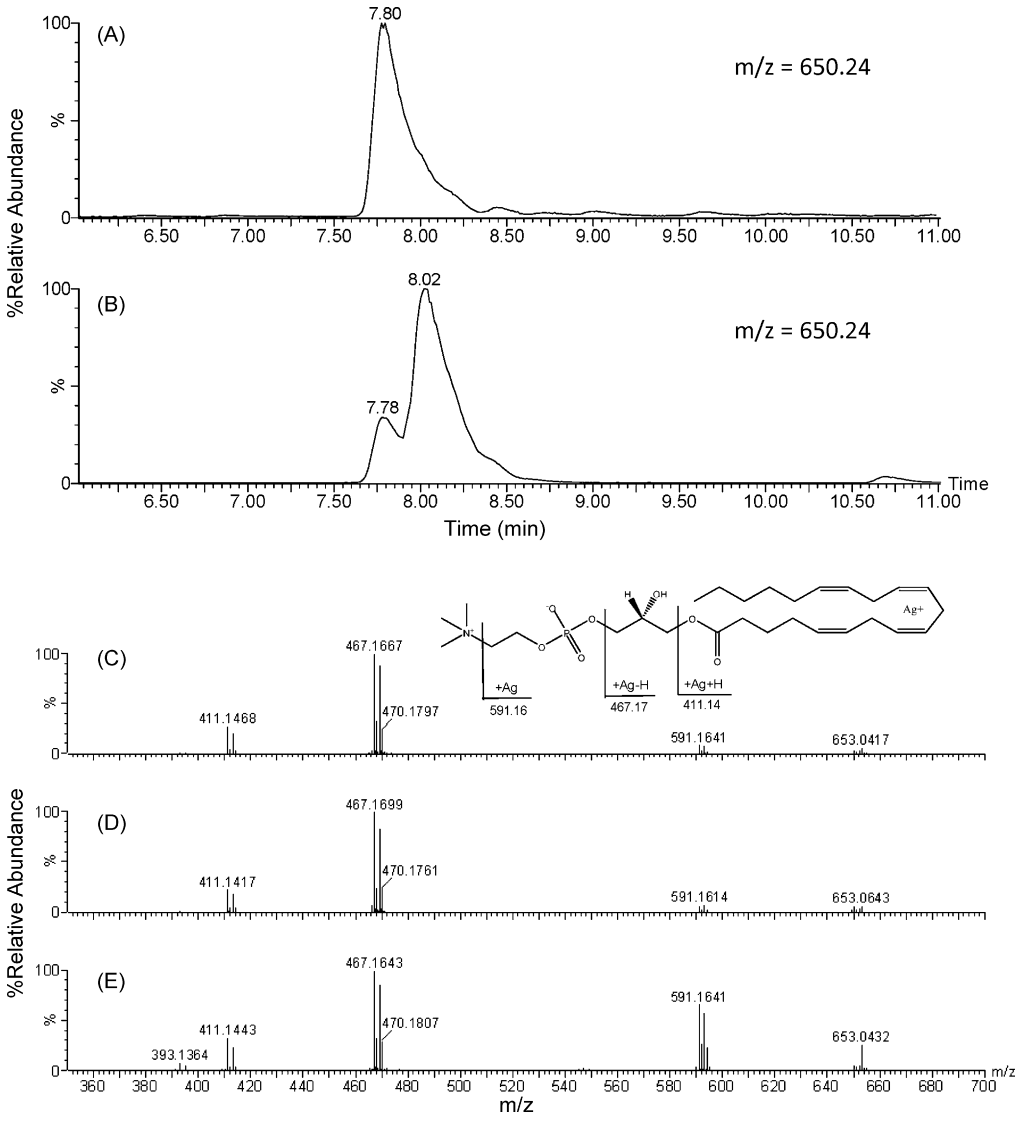

Fig. 4. (A) Selected ion chromatogram at 650.24 amu from whole mouse brain tissue. (B) Selected ion chromatogram at 650.24 amu of the synthesized 1-*O*-arachidonyl-*sn*-glycero-3-phosphocholine compound at 18.4 μM. (C) Fragmentation spectrum from the collisionally induced dissociation of the mouse brain compound seen at retention time 7.8 min. (D) Fragmentation spectrum from the collisionally induced dissociation of the 7.78 min peak from the 1-*O*-arachidonyl-*sn*-glycero-3-phosphocholine standard. (E) Fragmentation spectrum from the collisionally induced dissociation of the 8.02 min peak from the 1-*O*-arachidonyl-*sn*-glycero-3-phosphocholine standard. The difference in relative ion intensities between panels (D) and (E) is attributed to the presence of *sn*-2 product in the standard that has formed via acyl migration.

with [^{3}H] ARA compared to synthesis that is observed after [^{3}H] AEA pre-labeling [22]. Overall, our results indicate that cells have distinct mechanisms for handling lipid metabolites. Therefore, distinct pools of lipid metabolites may form depending on the source of the arachidonate chain and lipidomic profiling methodologies were developed and exploited to test this hypothesis.

Lipidomics or lipid profiling, a subclass of metabolomics, is a study of the lipid complement of a cell, tissue, or organism. In recent years, lipidomics has received increasing attention as a research tool in a range of diverse disciplines including physiology, lipid biochemistry, clinical biomarker discovery, and pathology [37]. The advancement of the field has been driven by the development of analytical technologies, and in particular advances in LC–MS. Stable isotope encoding may be implemented as a tool to study lipidomics and in our case measure the dynamics of the endocannabinoid metabolite pools.

As a general rule, stable isotope encoding strategies in concert with mass spectrometry can be used in the characterization of the molecular composition of protein, peptide, and lipid pools *in vitro* and *in vivo*. A common *in vitro* method of metabolic labeling involves feeding precursor metabolites to two populations of cultured cells that are labeled with isotopically distinct species that are otherwise structurally identical. At a defined stage of sample preparation before the mass spectrometric analysis, the samples are mixed, thus, becoming enriched in both the light and heavy isotopes. The technique of isotope encoding relies on the principle that molecules with the same chemical structure, differing only in their isotopic composition, will be processed by cells in a similar manner and respond equally if analyzed simultaneously using a mass spectrometer. If both of the cell populations, pre-labeled with light and heavy isotopes, are mixed in equal proportions, then during analysis, a series of doublets should be produced on the mass spectra. Doublets refer to pairs of peaks that correspond to the light and heavy isotopes and differ from each other by the mass units associated with the isotopes used.

Recent advances in the lipidomics field in concert with our newly developed LC–MS method allowed the study of endocannabinoid biotransformations by analyzing a large spectrum of

metabolites produced from AEA or ARA. We determined that lipids that are formed from AEA-derived arachidonate are different from non-AEA-derived arachidonate. Using the argentation approach we discovered that ARA-derived metabolites were comprised of one main lipid class—eicosanoids, whereas AEA-derived arachidonate, in addition to eicosanoids, was metabolized into diradylglycerols, fatty acid amides, sterols, and glycerophospholipids. The arachidonate chain is handled differently by the cell depending on the source of the lipid. This finding of differential metabolite handling may also explain why in the cellular model of endocannabinoid recycling, more AEA and 2-AG were produced from [^{3}H] ARA than from [^{3}H] AEA [22]. If ARA is recycled by the cell into a small subset of metabolites, then the ARA-containing pool is not exhausted because of the abundance of precursors. Furthermore, the result that AEA is recycled into a different set of metabolites compared with ARA, suggests that cells have a precise mechanism for directed trafficking of metabolites that depends on the identity and source of the parent compound. The hypothesis of directed trafficking of AEA lends support to the notion of a specific uptake process that directs the endocannabinoids to a cellular compartment that contains the specific metabolic enzymes.

Comparison of the metabolite peaks to peaks in unlabeled samples provided an indication of the baseline levels of the identified compounds. For those peaks in our labeled samples that had a height equal to the corresponding peak in the unlabeled samples (fatty acid amides, eicosanoids, phosphocholines, and diradylglycerols), we interpreted these as compounds that had rapid cellular turnover and were able to achieve steady-state levels over the course of the 24 h labeling period. For those compounds whose labeled peaks were less than the control peak heights (diradylglycerols and sterols), we suggest that the AEA treatment leads to altered cellular metabolic activity resulting in reduced levels in the labeled samples. One class of compounds, the fatty acid amides were found to have peak heights greater than those in the control samples. Because these compounds were all predicted to be fatty acid amides, we believe these compounds represent newly formed metabolites that may be the result of direct biotransformation of AEA itself by yet uncharacterized enzymes.

From the list of lipids that we identified as potential AEA metabolites, one lipid in particular was of interest to us because of its potential link to other biologically relevant lipid signaling molecules. The lipid was identified as 1-*O*-arachidonyl-*sn*-glycero-3-phosphocholine via the LipidMAPS database. After synthesizing a standard, we confirmed that the mass spectrometric properties of 1-*O*-arachidonyl-*sn*-glycero-3-phosphocholine matched the molecular weight, retention time, and fragmentation pattern (MS/MS) of the lipid that was identified using the lipid isotope encoding approach. These results indicate that a pathway may exist from d_8-AEA-derived arachidonate to 1-*O*-arachidonyl-*sn*-glycero-3-phosphocholine. Interestingly, our results are consistent with 2-*O*-arachidonyl-*sn*-glycero-3-phosphocholine being highly expressed endogenously in mouse brain tissue. If the *sn*-1 regioisomer is present in brain, it is a minor product as determined by comparison of the relative intensities of the product ions observed in the MS/MS analysis. Several questions still need to be addressed. For example, is the 1-*O*-arachidonyl-*sn*-glycero-3-phosphocholine molecule the metabolite of AEA or is the metabolite actually the *sn*-2 regioisomer? Also, can these acyl-phosphocholines serve as precursors in the biosynthesis of lipid-derived signaling molecules? Preliminary studies revealed that after treatment of RBL-2H3 cells with ionomycin, an agent that stimulates endocannabinoid biosynthesis, the levels of the 1-/or 2-*O*-arachidonyl-*sn*-glycero-3-phosphocholine increased compared to the untreated control (not shown). We recognize the nonspecific nature of the ionomycin treatment and therefore suggest the relationship between the acyl-glycero-3-phosphocholine and other lipid signaling molecules should be established in future studies using more specific approaches.

Although the formation of arachidonate-containing diacyl phospholipid molecules is well documented, it is unclear how arachidonate-containing lysolipids are formed. As a general rule, a diacyl phospholipid carries a saturated fatty acid at the *sn*-1 position, and the *sn*-2 position is acylated with a partially unsaturated fatty acid (such as arachidonic acid). The cellular biosynthetic mechanism for 1-*O*-arachidonyl-*sn*-glycero-3-phosphocholine formation is unknown. Possible mechanisms could include production of 1-*O*-arachidonyl-*sn*-glycero-3-phosphocholine by cellular *de novo* synthesis or via a transacylation process allowing the attachment of an AEA-derived arachidonate moiety to pre-existing phospholipids. Arachidonate moieties are usually expected to occupy the *sn*-2 position of a phospholipid, and the discovery here should stimulate the investigation whether an acyl rearrangement reaction is involved in the production of the arachidonyl-containing glycerol phosphocholine molecules.

5. Conclusions

We exploited silver coordination to the arachidonate chains of AEA and ARA to significantly improve sensitivity of the TOF mass analysis and achieve limits of detection and quantification comparable to that of triple quadrupole instruments. Argentation, or the use of silver coordination to organic molecules for detection improvement has been around since the 1930s. Winstein and Lucas were the first group to quantitatively characterize the nature of the interaction between silver ions and compounds that contained ethylenic or acetylenic bonds [38]. Thirty years later, the argentation approach became popular for separations of lipophilic materials [39]. Kingsley and Marnett reported that the limit of detection for endocannabinoids may be improved on the liquid chromatography mass spectrometry (LC–MS–MS) instruments by exploiting silver cation coordination to the arachidonate backbone of these eicosanoid molecules [23]. The electrons within the partially filled d-orbitals of silver coordinate to the π electrons in the double bonds within the arachidonate backbone of the neutral molecules, such as AEA and 2-AG, resulting in an $[M+Ag]^+$ species that easily undergo conversion to the gas phase via an electrospray ionization (ESI) source. The ease of analysis and specificity of the method makes this approach appealing for endocannabinoid quantification in our experimental setting. The silver-mediated enhancement of detection using a Q-TOF instrument now enables the accuracy and high throughput capacity of the TOF instrument to be used as a discovery tool for endocannabinoid metabolites (e.g., 1-*O*-arachidonyl-*sn*-glycero-3-phosphocholine). Such compound discovery efforts that require database searches, benefit from the higher mass accuracy of the TOF instrument as compared to triple quadrupole instruments. Once compounds of interest are identified, subsequent analyses of biological samples would benefit from the greater sensitivity of the triple quadrupole instrument. Together this approach could be used to identify and subsequently quantify various lipids in biological samples under various conditions (disease vs. normal, drug treated vs. untreated) providing important new information about biochemical and, in the case of the endocannabinoids, neurochemical changes that occur *in vivo*.

Acknowledgements

This work was supported by the National Institutes of Health grant R21 DA024193 (Eric Barker/V. Jo Davisson), R21 DA018112 (Eric Barker), and R33DK70290 (V. Jo Davisson). We thank Amber Hopf-Jannasch for help with XMASS analysis.

Appendix A. Supplementary data

Supplementary data associated with this article can be found, in the online version, at doi:10.1016/j.jpba.2010.03.035.

References

[1] S. Munro, K.L. Thomas, M. Abu-Shaar, Nature 365 (1993) 61–65.
[2] L.A. Matsuda, S.J. Lolait, M.J. Brownstein, A.C. Young, T.I. Bonner, Nature 346 (1990) 561–564.
[3] D. Smart, M.J. Gunthorpe, J.C. Jerman, S. Nasir, J. Gray, A.I. Muir, J.K. Chambers, A.D. Randall, J.B. Davis, Br. J. Pharmacol. 129 (2000) 227–230.
[4] P.M. Zygmunt, J. Petersson, D.A. Andersson, H. Chuang, M. Sørgård, V. Di Marzo, D. Julius, E.D. Högestätt, Nature 400 (1999) 452–457.
[5] V. Chevaleyre, K.A. Takahashi, P.E. Castillo, Ann. Rev. Neurosci. 29 (2006) 37–76.
[6] G. Di Carlo, A.A. Izzo, Expert Opin. Investig. Drugs 12 (2003) 39–49.
[7] M. Guzmán, Nat. Rev. Cancer 3 (2003) 745–755.
[8] D.M. Lambert, C.J. Fowler, J. Med. Chem. 48 (2005) 5059–5087.
[9] M.J. McFarland, A.C. Porter, F.R. Rakhshan, D.S. Rawat, R.A. Gibbs, E.L. Barker, J. Biol. Chem. 279 (2004) 41991–41997.
[10] M.J. McFarland, T.K. Bardell, M.L. Yates, E.A. Placzek, E.L. Barker, Mol. Pharmacol. 74 (2008) 101–108.
[11] B.F. Cravatt, A.H. Lichtman, Curr. Opin. Chem. Biol. 7 (2003) 469–475.
[12] D.G. Deutsch, S.A. Chin, Biochem. Pharmacol. 46 (1993) 791–796.
[13] V. Di Marzo, T. Bisogno, T. Sugiura, D. Melck, L. De Petrocellis, Biochem. J. 331 (1998) 15–19.
[14] S.K. Goparaju, N. Ueda, H. Yamaguchi, S. Yamamoto, FEBS Lett. 422 (1998) 69–73.
[15] V. Di Marzo, Biochim. Biophys. Acta 1392 (1998) 153–175.
[16] K.R. Kozak, B.C. Crews, J.D. Morrow, L.H. Wang, Y.H. Ma, R. Weinander, P.J. Jakobsson, L.J. Marnett, J. Biol. Chem. 277 (2002) 44877–44885.
[17] A.J. Hampson, W.A. Hill, M. Zan-Phillips, A. Makriyannis, E. Leung, R.M. Eglen, L.M. Bornheim, Biochim. Biophys. Acta 1259 (1995) 173–179.
[18] N.T. Snider, A.M. Kornilov, U.M. Kent, P.F. Hollenberg, J. Pharmacol. Exp. Ther. 321 (2007) 590–597.
[19] P.J. Kingsley, L.J. Marnett, J. Chromatogr. B. Anal. Technol. Biomed. Life Sci. 877 (2009) 2746–2754.
[20] E. London, D.A. Brown, Biochim. Biophys. Acta 1508 (2000) 182–195.
[21] L.J. Pike, X. Han, K.N. Chung, R.W. Gross, Biochemistry 41 (2002) 2075–2088.
[22] E.A. Placzek, Y. Okamoto, N. Ueda, E.L. Barker, J. Neurochem. 107 (2008) 987–1000.
[23] P.J. Kingsley, L.J. Marnett, Anal. Biochem. 314 (2003) 8–15.
[24] X. Zhang, W. Hines, J. Adamec, J.M. Asara, S. Naylor, F.E. Regnier, J. Am. Soc. Mass Spectrom. 16 (2005) 1181–1191.
[25] J. Lindberg, J. Ekeroth, P. Konradsson, J. Org. Chem. 67 (2002) 194–199.
[26] B. Tan, H.B. Bradshaw, N. Rimmerman, H. Srinivasan, Y.W. Yu, J.F. Krey, M.F. Monn, J.S. Chen, S.S. Hu, S.R. Pickens, J.M. Walker, AAPS J. 8 (2006) E461–E465.
[27] M. Palkovits, J. Harvey-White, J. Liu, Z.S. Kovacs, M. Bobest, G. Lovas, A.G. Bago, G. Kunos, Neuroscience 152 (2008) 1032–1039.
[28] C.C. Felder, A. Nielsen, E.M. Briley, M. Palkovits, J. Priller, J. Axelrod, D.N. Nguyen, J.M. Richardson, R.M. Riggins, G.A. Koppel, S.M. Paul, G.W. Becker, FEBS Lett. 393 (1996) 231–235.
[29] D. Richardson, C.A. Ortori, V. Chapman, D.A. Kendall, D.A. Barrett, Anal. Biochem. 360 (2007) 216–226.
[30] T. Bisogno, F. Berrendero, G. Ambrosino, M. Cebeira, J.A. Ramos, J.J. Fernandez-Ruiz, V. Di Marzo, Biochem. Biophys. Res. Commun. 256 (1999) 377–380.
[31] T. Sugiura, S. Kondo, A. Sukagawa, S. Nakane, A. Shinoda, K. Itoh, A. Yamashita, K. Waku, Biochem. Biophys. Res. Commun. 215 (1995) 89–97.
[32] N. Stella, P. Schweitzer, D. Piomelli, Nature 388 (1997) 773–778.
[33] D. Piomelli, Nat. Rev. Neurosci. 4 (2003) 873–884.
[34] E.L. Barsumian, C. Isersky, M.G. Petrino, R.P. Siraganian, Eur. J. Immunol. 11 (1981) 317–323.
[35] E.A. Placzek, Y. Okamoto, N. Ueda, E.L. Barker, Neuropharmacology 55 (2008) 1095–1104.
[36] F. Rakhshan, T.A. Day, R.D. Blakely, E.L. Barker, J. Pharmacol. Exp. Ther. 292 (2000) 960–967.
[37] L.D. Roberts, G. McCombie, C.M. Titman, J.L. Griffin, J. Chromatogr. B. Anal. Technol. Biomed. Life Sci. 871 (2008) 174–181.
[38] S. Winstein, H.J. Lucas, J. Am. Chem. Soc. 60 (1938) 152–155.
[39] L.J. Morris, J. Lipid Res. 7 (1966) 717–732.